Title

Epoxy resin reinforced with nanothin polydopamine-coated carbon nanotubes: a study of the interfacial polymer layer thickness

Journal

RSC Advances, 6(37)

ISSN

2046-2069

Authors

Ling, Yang
Li, Weizhen
Wang, Baoyu
et al.

Publication Date

2016

DOI

10.1039/c5ra26539h

Peer reviewed

Epoxy resin reinforced with nanothin polydopamine-coated carbon nanotubes: A study of the interfacial polymer layer thickness

Yang Ling, Weizhen Li*, Baoyu Wang, Wenjun Gan*
[1]Department of Macromolecular Materials and Engineering, College of Chemistry and Chemical Engineering, Shanghai University of Engineering Science, 201620, Shanghai, China

Chenhui Zhu, Michael A. Brady, Cheng Wang
[2]Advanced Light Source, Lawrence Berkeley National Laboratory, 1 Cyclotron Road, Berkeley, CA 94720, USA

Correspondence to: W. Z. Li (Email: liweizhen@sues.edu.cn); W. J. Gan (Email: wjgan@sues.edu.cn)

ABSTRACT: Carbon nanotubes (CNTs) functionalized by a nanothin poly(dopamine) (PDA) layer were produced by a one-pot, nondestructive approach, with direct polymerization of dopamine on the CNT surface. The thickness of the PDA layer can be well-controlled by the reaction time and the proportion of dopamine, and this thickness is found to be the key factor in controlling the dispersion of CNTs and the extent of the interfacial interactions between the CNTs@PDA and epoxy resin. SEM results indicated that the dispersion of CNTs in epoxy was improved significantly by coating a nanothin PDA layer onto the CNT surface. In agreement with this finding, the CNTs funtionalized with the thinnest PDA layer provided the best mechanical and thermal properties. This result confirmed that a thinner PDA layer could provide optimized interfacial interactions between the CNTs@PDA and epoxy matrix and weaken the self-agglomeration of CNTs, which led to an improved effective stress and heat transfer between the CNTs and polymer matrix.

Key words: epoxy resin, polydopamine, carbon nanotubes, core-shell structure, surface functionalization

1. INTRODUCTION

As high performance carbon nanomaterials, carbon nanotubes (CNTs) have attracted intense attention to be promising reinforcing fillers for polymer matrices[1-3], because of their outstanding properties, like low density, high aspect ratio, and superior physical[4,5], electrical[6,7] and thermal potentials[8,9]. However, the agglomeration of the CNTs, owing to the high Van der Waals attraction between tubes, has been considered as the main hurdle for effective reinforcement in polymer composites, which is also the result of weak interfacial adhesion between the CNTs and the polymer matrix. Therefore, the surface modification or functionalization of CNTs has become a major research activity within nanoscience, nanotechnology, and bioengineering, as the best approach for improving the solubility and compatibility of CNTs in polymer matrices. Non-covalent and covalent modifications of the CNT surface have both been used previously to enhance the dispersion and processability of CNTs in common solvents and blended composites, including oxidative processes with strong acid[10], introducing active functional groups[11], functional coatings by the sol-gel method[12], grafting polymer by surface-initiated polymerization[13,14], among others. However, most modification methods have major drawbacks with the surface destruction and fragmentation into smaller pieces by concentrated acid and strong oxidation processes, which are both environmentally unfriendly. Therefore, many efforts have been put forward to develop methods that are industrially relevant to use, of low cost, and less destructive to the CNT surface structure. Among the low-damage methods, polymer wrapping and “pi-pi” stacking on the surface of CNTs resulted in good dispersibility in aqueous solutions, but they are difficult to process once within the polymer matrix due to the slippage of the stacked molecules.

Recently, self-polymerization of organic monomers onto the convex walls of CNTs has been demonstrated as an effective approach to generate specific coatings, especially polydopamine (PDA) coatings. Lee *et al.*[15] reported that the adhesive proteins secreted by mussels (PDA) can self-polymerize via a simple deposition

process under alkaline conditions and attach the adhesive layer onto almost all types of surface, be it organic or inorganic. In the past years, a large amount of substrates have been functionalized with polydopamine, such as electrospun nanofibers[16-18], clay[19-21], carbon fiber[22] and graphene oxide[23-25]. As a non-covalent modification method, the PDA functionalization process has significant advantages, like high efficiency, ease of procedure, and mild reaction conditions, exclusive from concentrated acid and strong oxidation processes. Furthermore, the PDA coating layer could also act as a multipurpose platform for secondary reactions or further improvement of surface functionality, such as immobilization of various organic species at the surface [26-30].

Previous research has illustrated that the PDA-mediated nanomaterials are advantageous for their application in hydrophilic matrices, like polar solutions, aqueous environments, and biologically relevant surroundings [31-34]. Further applications were shown in a polymer matrix by Feng *et al.*[22], where carbon fibers modified with PDA films, to control hydrophilic and oleophilic surface behavior, resulted in an excellent interfacial improvement in the epoxy and poly(ethylene-*co*-octene) matrix. Lu *et al.* developed PDA-coated clay to improve the thermomechanical properties of the epoxy resin at very low inorganic loadings [21]. To the best of our knowledge, few reports have focused on the surface functionalization of CNTs via dopamine and on the improvement of interfacial adhesion between CNTs and the hydrophilic polymer matrix.

Inspired by the above mentioned, a one-pot, low cost and efficient PDA-coating method for CNTs was developed in this present work. This functionalization method is under alkaline conditions, with a simple deposition process that is environmental friendly and does not damage the nanotube sidewall, which commonly occurs with concentrated acid and strong oxidation processes. The process of functionalization of the CNTs and the formation of epoxy composites are shown in Scheme 1. The as-prepared CNTs@PDA/epoxy composites exhibited significant improvements in mechanical properties as a result of enhanced interfacial interactions, produced by the

combined mechanisms of hydrogen bonding between amine and hydroxyl groups of PDA and abundant hydroxyl groups of epoxy resin, and polymer entanglement between epoxy and PDA. It is worth noting that the amide-rich surface of PDA-coated CNTs may have a tendency to form aggregates via hydrogen bonding during the curing reaction, which would restrict their dispersion. In this study, this disadvantage was avoided by optimizing the thickness of the PDA layer, which was well controlled by the concentration of dopamine and the reaction time. The effect of the PDA layer thickness on the improvements of the composites performance is also investigated and presented, such as storage modulus, thermal stability, and thermal conductivity.

2. EXPERIMENTAL SECTION

2.1 Materials

Pristine multi-walled carbon nanotubes (CNTs), with a mean diameter of 20-40 nm and a length of 5-15 μm, were supplied by Nanotech Port Co., Ltd. (Shenzhen, China). Dopamine (DOPA, 99%) was purchased from Alfa Aesar (USA). Bisphenol A diglycidyl ether (DGEBA) was supplied by Dow Chemical (USA). Tris(hydroxymethyl)aminomethane (TRIS), N,N-dimethylbenzylamine, and methyltetrahydrophthalic anhydride (Me-THPA) were provided by Sinopharm Chemical Reagent Co., Ltd (China). Other reagents were of analytical grade or better and used without further purification.

2.2 CNTs modified by poly(dopamine) (CNTs@PDA)

100 mg of CNTs was dispersed in a mixed solution of ethanol (50 ml) and water (40 ml) under ultrasonication for 45 min. Then, 400 mg of DOPA (4:1 DOPA:CNTs by wt.) was added under magnetic stirring for 5 min. Next, 100 ml of aqueous solution of TRIS (300 mg) was added, and the solution was stirred for 24 h at ambient temperature. The product was collected by filtration and washed with deionized water and ethanol until the scrubbing filtrate became colorless, and then finally dried in vacuum oven at 80 ºC overnight. The resultant material is defined as CNTs@PDA-a. In order to control the coverage thickness, the DOPA concentration and the reaction

time was changed. CNTs@PDA-b (1:1 DOPA:CNTs by wt.) was prepared by the same procedure except using a decreased amount of DOPA (100 mg); CNTs@PDA-c (DOPA:CNTs = 0.5:1) was prepared similarly but with 50 mg of DOPA and with a reduced reaction time of 12 h. Finally, pure poly(dopamine) (PDA) was produced in the same manner except without addition of CNTs.

2.3 Preparation of CNTs/epoxy Composites

Me-THPA and N,N-dimethylbenzylamine were mixed in the proportion of 80:0.2 by wt. to obtain the curing agent mixture. A desired amount (0.5 wt. %, 0.75 wt. %, 1 wt. %, 1.5 wt. %, 2 wt. %, and 3 wt. %) of CNTs and the above curing agent were first added in a beaker, and the mixture was heated and kept at 50 ºC for 30 min under ultrasonication. Next, DGEBA was added, and all components were uniformly mixed together at 50 ºC with ultrasonication for 30 min. Finally, the mixture was poured into a home-made mold. All samples were cured at 150 ºC for 5 h and 200 ºC for 2h. The CNTs@PDA/epoxy nanocomposite was prepared by the same procedure.

2.4 Characterization

Fourier transform infrared spectroscopy (FTIR) was conducted on a Nicolet AVATAR (Thermo Fisher, USA), with a resolution of 4 cm^{-1}. X-ray diffraction (XRD) patterns were measured using a CuKα source (λ=0.154nm) operating at 100 mA and 40 kV and a wide-angle analyzer, D/max-2500PC (Bruker, USA). Thermal gravimetric analysis (TGA) was performed on a PT 1000 (Linseis, Germany). The surface morphology of CNTs was observed by transmission electron microscopy (TEM, JEOL JEM2100F). Scanning electron microscopy (SEM, HITACHI SU8010) was applied to observe the fracture surface of the composites. Dynamic mechanical analysis (DMA) was performed using a DMA Q800 (TA Instruments, USA), over a temperature range of 30-180 ºC and at a frequency of 1 Hz. The thermal conductivity of composites was measured by a DRL-2B instrument name? (Xiangtan Instrument Co., Ltd. China).

Small-Angle X-ray Scattering (*SAXS*) *and Wide-Angle X-ray Scattering* (*WAXS*). SAXS and WAXS experiments were performed at beamline 7.3.3 at the Advanced Light Source (ALS) of Lawrence Berkeley National Laboratory. The fully cured samples were fixed with Kapton tape. An X-ray energy of 10 keV (λ=1.24 Å) was used, and the 2D scattering images were collected on a Pilatus 1M detector at room temperature. A silver behenate sample was used for the calibration of the sample-to-detector distance.

3. RESULTS AND DISCUSSION

3.1 Surface functionalization and characterization of CNTs

The synthetic approach of CNTs@PDA nanocomposites is highly reproducible, and the as-prepared CNTs@PDA has shown good and stable dispersibility in polar solvents, like water, ethanol, and tetrahydrofuran. Additionally, the synthetic process presented in this report allows for facile control over the PDA shell thickness. Direct evidence for the successful surface functionalization of CNTs was provided by TEM, as shown in Fig. 1. Compared with the pristine CNTs of Fig.1a, it can be obviously observed that PDA layers are uniformly coated on the surface of CNTs, resulting in core-shell cable-like CNTs@PDA in Fig. 1b and c. In addition, the shell thickness gradually decreases from 25 nm to 10 nm, with decreasing the mass ratio of DOPA and CNTs from 4:1 to 1:1 (Fig.1b and c). Fig. 1c especially shows a clear boundary between the PDA layer and the multi-walled CNTs. With further reduction in the reaction time and the mass ratio of DOPA and CNTs to 0.5:1, a nano-thin layer of PDA (below 5 nm) can be observed in Fig. 1d. According to the above conclusions, CNTs@PDA-a, CNTs@PDA-b, and CNTs@PDA-c with different thickness layers were defined as CNTs@PDA-25, CNTs@PDA-10, and CNTs@PDA-5 in the following sections. It can be concluded that the thickness of the PDA shell can be easily controlled by changing the mass ratio of DOPA and CNTs and the reaction time whilst keeping the other synthetic parameters constant.

More evidence of the existence of the PDA shell can be provided by FTIR analysis, as shown in Fig. 2. The dopamine spectrum shows features of catechol

groups at 3040 and 3246 cm^{-1}, a sharp peak at 1287 cm^{-1} representing the C-O stretching vibration, and the characteristic peak of aromatic rings at 1620 cm^{-1}. After polymerization, PDA displays intense absorption peaks at 1287 and 1620 cm^{-1} and a broad peak at 3403 cm^{-1}, attributed to C-O stretching vibration, the aromatic rings, and the merging of -OH and –NH features, respectively. For the pristine CNTs, there are nearly no peaks observed except a weak feature at 1578 cm^{-1}, which is related to the structure of the graphite tube wall of multi-walled carbon nanotubes[35]. After coating with PDA by the oxidative self-polymerization, the as-prepared CNTs@PDA show clear absorption peaks at 1620 and 3458 cm^{-1}, signifying the existence of O-H and N-H, respectively, stretching vibration from the PDA layer[36]. Therefore, FTIR analysis confirms the uniform coating of the CNTs by PDA formed during the oxidative interfacial polymerization process.

XRD patterns of pristine CNTs, CNTs@PDA-25, CNTs@PDA-10, and CNTs@PDA-5 are presented in Fig. 3. It can be observed that the main XRD features of pristine CNTs are at 2θ= 26° (*(002)*), 42.5° (*(100)*), and 53.5° (*(004)*)[37]. In the XRD pattern of the CNTs@PDA composites, the above corresponding peaks are weakened when increasing the PDA layer thickness from CNTs@PDA-5 to CNTs@PDA-25. This also proves the success of the surface functionalization and that the coating layer thickness increased with the concentration of DOPA.

TGA analysis also verified the difference in the thickness of the PDA layer, as shown in Fig. 4. Pristine CNTs undergo only 5 wt. % loss at temperatures up to 800 ºC. After modification with PDA-5, a 5 wt. % loss is found at 401 ºC. As expected, CNTs@PDA-10 and CNTs@PDA-25 show 5 wt. % loss at lower temperatures, at 279ºC and 234ºC, respectively. Pure PDA displayed approximately 56% weight loss at temperatures up to 700 ºC. Based on the differences in thermal stability among the PDA-coated CNTs, it can be inferred that the coating thickness increases with PDA concentration. This result thus indicates that a range of coating layer thicknesses can be obtained by controlling the polymerization conditions.

3.2 Dynamic mechanical properties of composites

Pristine CNTs are highly hydrophobic, inducing poor dispersibility in polar solvents and hydrophilic polymers, such as epoxy resins. To solve this problem, the modification of the CNT surface by a nanothin PDA layer was performed in this study. Compared with methods involving oxidation of CNTs, the PDA coating process will retain the inherent properties of the pristine CNTs without disturbing their structure and provide a more compatible interface between the CNTs and polymer matrix. In this regard, DMA is a powerful tool to investigate the mechanical properties of polymers, the results of which are highly relevant to and indicative of the dispersion of the nanofillers and their interactions with the polymer matrix.

The DMA results for each composite are given in Fig. 5, and the calculated values of the glass transition temperature (T_g) are listed in Table 1 for comparison. Fig. 5a shows that the introduction of CNTs in the epoxy resin caused an increase of storage modulus (E') below T_g, which can be explained as CNTs behaving as an obstacle to the molecular chains of epoxy[38]. However, the increase of the storage modulus is limited, and the maximum increase is 9 %. Compared with the composites with pristine CNTs, CNTs@PDA/epoxy composites show a significant enhancement of E' at very low CNTs@PDA loading. Especially for the composites with the thinnest PDA layer, seen in Fig.5 d, the storage modulus increases ~29 % at room temperature from 2.72 GPa for neat epoxy to 3.50 GPa for the composites with a 1.5 wt. % loading of CNTs@PDA-5. For the CNTs@PDA with a thicker PDA layer, the maximum enhancement of the storage modulus of CNTs@PDA/epoxy composites can also be obtained with a loading of 1.5 wt. % CNTs@PDA-25 and CNTs@PDA-10, of 18 % and 22 %, respectively.

To date, it is believed that numerous amine and catechol functional groups are present in the PDA coating. The reinforcement effect of CNTs@PDA composites is mainly thought to be due to the enhanced interfacial interaction between the catechol groups at the CNTs@PDA surface and the epoxy matrix. Therefore, the stiffness of the CNTs@PDA/epoxy composites can be improved significantly at very low CNTs

loadings, owing to the more effective stress transfer from high modulus CNTs to the polymer matrix. Moreover, the amine groups of the PDA may also help in accelerating the curing reaction of DGEBA, which leads to better compatibility between the functionalized CNTs and DGEBA. Is this due to better dispersibility or what causes the amine groups to improve the compatibility?

For the composites with different thickness of the PDA layer, all storage modulus values of CNTs@PDA-5 are higher than those of CNTs@PDA-25 and CNTs@PDA-10, owing to its thinnest coating layer. The cause of this thickness-dependent behavior is related to the dispersion of the CNTs@PDA within the epoxy matrix. It can be hypothesized that a large number of catechol and amine groups on the surface of coating not only promote the dispersion of CNTs but also act as bridges between the adjacent CNTs. That bridging behavior leads to self-agglomeration of CNTs@PDA, which would cause aggregate formation in the epoxy composites. These defects can act as stress concentration points within the material and cause the observed reduction in storage modulus (Is this right?). When the curvature of the functionalized CNTs was changed due to the coating of a thicker PDA layer, the bridges between the adjacent CNTs increased, and therefore the CNTs aggregated significantly, which can be observed in SEM (Fig. 6).

As a result, the CNTs@PDA-5/epoxy composites showed the highest storage moduli. There is, however, a maximum loading for CNTs@PDA-5 of 1.5 wt. %. With increasing the loading of the functionalized CNTs to 2 – 3 wt. %, the storage modulus decreased because of the agglomeration of CNTs.

In addition, the T_g of epoxy composites decreased with the addition of both the pristine CNTs and CNTs@PDA. As literature suggests[39], the reduction in T_g of nanofiller/epoxy composites could be related to that the unfavorable interactions at the polymer matrix-hard surface interface, although there is slightly compatible PDA coating covered on CNTs surface in this study. This unfavorable interactions lead to immobile domains in the epoxy matrix, thus causing a drop in the T_g value. On the other hand, this effect would be weakened for the composites containing aggregated

CNTs. Based on the T_g results of CNTs@PDA/epoxy system, the amine-groups of PDA surface had not obviously influence on the curing reaction of the epoxy resin.

3.3 Morphology of epoxy nanocomposites

Analysis of the fracture surfaces of different CNTs/epoxy nanocomposites is shown in Fig. 6. As indicated in Fig. 6a and b, the fracture surface of neat epoxy exhibits a smooth and flat surface with the linear cracks that are uniformly ordered, exhibiting a typical brittle fracture feature. In Fig. 6c and d, no obvious distinction can be observed between the neat epoxy and the pristine CNTs/epoxy composites except for the big agglomerations of pristine CNTs. Further, Fig.6d shows that the direction of cracks on the fracture surface becomes unordered. For the composites with CNTs@PDA, the fracture surface becomes rougher, and a large area of unordered cracks appears, seen in Fig. 6e and g. This fracture behavior may be attributed to the presence of strong interfacial interactions between the funtionalized CNTs and epoxy matrix, inducing more effective stress transfer between the polymer matrix and the high modulus CNTs, restraining the large-scale crack growth in the matrix, therefore making the surface more rough. The fracture behavior proves that the addition of the PDA-functionalized CNTs does improve the toughness of epoxy matrix. The distinction in the dispersion of pristine CNTs, CNTs@PDA-25/EP, and CNTs@PDA-5/EP can be observed in Fig. 6d, f, and h. CNTs covered by the thinnest PDA layer show the best dispersibility in the epoxy matrix. Thus, the storage modulus of CNTs@PDA composites can be improved significantly and most effectively with CNTs@PDA-5 loading.

3.4 Thermal stability and thermal conductivity of epoxy nanocomposites

The thermal stability of epoxy composites is presented in Fig. 7. It can be observed that TGA curves of neat epoxy and CNTs/EP composite show almost no distinction. Compared with the neat epoxy and pristine CNTs/epoxy composite, CNTs@PDA-25/epoxy and CNTs@PDA-10/epoxy composites show slightly lower

degradation onset temperatures, which is due to the poorer thermal stability of the PDA coating layer. However, the CNTs@PDA-5/epoxy composite shows a higher onset degradation temperature. $T_{95wt\%}$ (temperature corresponding to 5 % weight loss) for all of the epoxy composites is listed in Table 2. The $T_{95wt\%}$ of CNTs@PDA/epoxy composites increases with reduction in the PDA layer thickness. The best dispersion of CNTs@PDA-5 in epoxy matrix could be an additional reason for the enhanced thermal stability of the epoxy composites.

The room-temperature thermal conductivity of neat epoxy and CNTs/epoxy composites was also investigated, and the results are shown in Fig. 8. For all samples, the thermal conductivity of CNTs@PDA/epoxy increases with increasing concentration of filler. The thermal conductivity for neat epoxy is 0.22 W/m-K, while for the epoxy with 3 wt. % pristine CNTs and 3 wt. % CNTs@PDA-5, the value increases to 0.30 and 0.34 W/m-K, respectively. For the composites containing CNTs with a thicker PDA layer (CNTs@PDA-25 and CNTs@PDA-10), however, the thermal conductivity is lower than in the pristine CNTs/epoxy composites. The improvement by the thinner PDA layer (CNTs@PDA-5) is explained by the stronger interfacial interaction between the CNTs and epoxy for thin PDA layers which could decrease the scattering for the heat carrying wave package (phonon) transfer, therefore increasing the thermal conductivity, but this thermal conductivity enhancement is also strongly related to a better dispersion in the epoxy. The agglomerations in the CNTs@PDA-25 and CNTs@PDA-10 composites cause increased phonon scattering, which restricts the diffusion of heat flow in the CNTs/epoxy composites[40].

Small angle X-ray scattering (SAXS) and wide angle X-ray scattering (WAXS) were carried out to study the effects of MWCNTs and the thickness of PDA coating on the microstructure of composites. The scattering peak position of the SAXS reflects the average center-to-center distance of adjacent high and low density regions [41]. There is no SAXS peak for the neat epoxy resin; only a monotonically decreasing scattering profile was observed. The absence of peaks for the blends

studied here (Fig. 9a) may indicate a homogeneous blend on length scales of 3 – 150 nm. For CNTs/epoxy composites, there is a broad feature centered at q =0.0305 (20.6 nm). This feature originates from the characteristic length scale of the dispersion, with CNT-rich regions being spaced by approximately 20 nm.

For WAXS measurements shown in Fig 9b, except for the peak at q = 0.40 Å $^{-1}$ from the Kapton window and small peak at q = 1.844 Å $^{-1}$ from the CNT tube structure, another two obvious broad peaks appear for all samples. For the neat DGEBA epoxy resin, two well-defined maxima in the scattering profile were seen at 0.456 Å $^{-1}$ and 1.19 Å $^{-1}$, corresponding to a periodicity of 13.8 Å and 5.3 Å, consistent well with the anhydride-cured systems where two comparatively wide maxima were distinguished in the diffractograms corresponding to Bragg distances 13.5 and 5.1 Å for DGEBA-HHPA (hexahydrophthalic anhydride) [42] and 2θ =17.3° (q = 1.23 Å^{-1}) for MeTHPA-cured neat epoxy [43]. For the low angle peak 0.456 Å $^{-1}$, we assign it as originating from the isopropylidene group -C(CH_3)$_2$- in DGEBA. Moreover, there is a trend in the intensity of the high-angle peaks, increasing with the introduction of MWCNTs of low PDA coating thickness, implying that the stacking behavior of molecular groups within the epoxy changes during the curing reaction of epoxy resin and is affected by the presence of the filler nanotubes.

4. CONCLUSIONS

A non-covalent, one-pot interfacial polymerization method has been shown to create a strong interfacial interaction between CNTs and epoxy resin by self-polymerization of dopamine at the CNTs surface. The synthetic approach of CNTs@PDA is highly reproducible and allows facile control over the thickness of the PDA layer by the proportion of dopamine and reaction time. By using these CNTs functionalized with a nanothin PDA layer (<5 nm), the dispersion of CNTs in the epoxy matrix can be significantly improved. The nanothin PDA layer is believed to play a role of interfacial bonding via hydrogen bonding between amine and hydroxyl groups of PDA and hydroxyl groups of epoxy. These improved interfacial interactions

lead to simultaneous improvements in storage modulus, thermal stability, and thermal conductivity with the addition of CNTs@PDA. As for the influence of PDA layer thickness, the composite with the thinnest PDA layer shows the highest effective reinforcement and the best thermal conductivity for the epoxy composite.

References

[1] Cadek M, Coleman J, Ryan K, Nicolosi V, Bister G, Fonseca A, et al. Reinforcement of polymers with carbon nanotubes: the role of nanotube surface area. Nano Letters. 2004; 4(2): 353-356.

[2] Coleman JN, Blau WJ, Dalton AB, Munoz E, Collins S, Kim BG, et al. Improving the mechanical properties of single-walled carbon nanotube sheets by intercalation of polymeric adhesives. Applied Physics Letters. 2003; 82(11): 1682-1684.

[3] Gao J, Zhao B, Itkis ME, Bekyarova E, Hu H, Kranak V, et al. Chemical engineering of the single-walled carbon nanotube-nylon 6 interface. Journal of the American Chemical Society. 2006; 128(23): 7492-7496.

[4] Goze C, Vaccarini L, Henrard L, Bernier P, Hemandez E, Rubio A. Elastic and mechanical properties of carbon nanotubes. Synthetic Metals. 1999; 103(1): 2500-2501.

[5] Ruoff RS, Qian D, Liu WK. Mechanical properties of carbon nanotubes: theoretical predictions and experimental measurements. Comptes Rendus Physique. 2003; 4(9): 993-1008.

[6] Dai H, Wong EW, Liebert CM. Probing electrical transport in nanomaterials: conductivity of individual carbon nanotubes. Nature. 1996; 384: 147-150.

[7] Okuyama H, Iwata N, Yamamoto H. Position-selective growth of vertically aligned carbon nanotubes for application of electronic-measuring nanoprobes. Physica E: Low-dimensional Systems and Nanostructures. 2007; 37(1): 49-53.

[8] Liu Z-H, Yang X-F, Guo G-L. Influence of carbon nanotube suspension on the thermal performance of a miniature thermosyphon. International Journal of Heat and Mass Transfer. 2010; 53(9): 1914-1920.

[9] Xue H, Fan J, Hu Y, Hong R, Cen K. The interface effect of carbon nanotube suspension on the thermal performance of a two-phase closed thermosyphon. Journal of Applied Physics. 2006; 100(10): 104909.

[10] Esumi K, Ishigami M, Nakajima A, Sawada K, Honda H. Chemical treatment of carbon nanotubes. Carbon. 1996; 34(2): 279-281.

[11] Mickelson E, Huffman C, Rinzler A, Smalley R, Hauge R, Margrave J. Fluorination of single-wall carbon nanotubes. Chemical Physics Letters. 1998; 296(1): 188-194.

[12] Guo J, Saha P, Liang J, Saha M, Grady BP. Multi-walled carbon nanotubes coated by multi-layer silica for improving thermal conductivity of polymer composites. Journal of Thermal Analysis and Calorimetry. 2013; 113(2): 467-474.

[13] Sakellariou G, Priftis D, Baskaran D. Surface-initiated polymerization from carbon nanotubes: strategies and perspectives. Chemical Society Reviews. 2013; 42(2): 677-704.

[14] Yadav SK, Mahapatra SS, Cho JW, Lee JY. Functionalization of multiwalled carbon nanotubes with poly(styrene-b-(ethylene-co-butylene)-b-styrene) by click coupling. The Journal of Physical Chemistry C. 2010; 114(26): 11395-11400.
[15] Lee H, Dellatore SM, Miller WM, Messersmith PB. Mussel-inspired surface chemistry for multifunctional coatings. Science. 2007; 318(5849): 426-430.
[16] Son HY, Ryu JH, Lee H, Nam YS. Silver-Polydopamine hybrid coatings of electrospun poly (vinyl alcohol) nanofibers. Macromolecular Materials and Engineering. 2013; 298(5): 547-554.
[17] Son HY, Ryu JH, Lee H, Nam YS. Bioinspired templating synthesis of metal–polymer hybrid nanostructures within 3D electrospun nanofibers. ACS Applied Materials & Interfaces. 2013; 5(13): 6381-6390.
[18] Rim NG, Kim SJ, Shin YM, Jun I, Lim DW, Park JH, et al. Mussel-inspired surface modification of poly (l-lactide) electrospun fibers for modulation of osteogenic differentiation of human mesenchymal stem cells. Colloids and Surfaces B: Biointerfaces. 2012; 91: 189-197.
[19] Phua SL, Yang L, Toh CL, Guoqiang D, Lau SK, Dasari A, et al. Simultaneous enhancements of UV resistance and mechanical properties of polypropylene by incorporation of dopamine-modified clay. ACS Applied Materials & Interfaces. 2013; 5(4): 1302-1309.
[20] Phua SL, Yang L, Toh CL, Huang S, Tsakadze Z, Lau SK, et al. Reinforcement of polyether polyurethane with dopamine-modified clay: the role of interfacial hydrogen bonding. ACS Applied Materials & Interfaces. 2012; 4(9): 4571-4578.
[21] Yang L, Phua SL, Teo JKH, Toh CL, Lau SK, Ma J, et al. A biomimetic approach to enhancing interfacial interactions: polydopamine-coated clay as reinforcement for epoxy resin. ACS Applied Materials & Interfaces. 2011; 3(8): 3026-3032.
[22] Chen S, Cao Y, Feng J. Polydopamine as an efficient and robust platform to functionalize carbon fiber for high-performance polymer composites. ACS Applied Materials & Interfaces. 2013; 6(1): 349-356.
[23] Tian Y, Cao Y, Wang Y, Yang W, Feng J. Realizing ultrahigh modulus and high strength of macroscopic graphene oxide papers through crosslinking of mussel-inspired polymers. Advanced Materials. 2013; 25(21): 2980-2983.
[24] Kaminska I, Das MR, Coffinier Y, Niedziolka-Jonsson J, Sobczak J, Woisel P, et al. Reduction and functionalization of graphene oxide sheets using biomimetic dopamine derivatives in one step. ACS Applied Materials & Interfaces. 2012; 4(2): 1016-1020.
[25] Xu LQ, Yang WJ, Neoh K-G, Kang E-T, Fu GD. Dopamine-induced reduction and functionalization of graphene oxide nanosheets. Macromolecules. 2010; 43(20): 8336-8339.
[26] Sa R, Yan Y, Wei Z, Zhang L, Wang W, Tian M. Surface modification of aramid fibers by bio-Inspired poly(dopamine) and epoxy functionalized silane grafting. ACS Applied Materials & Interfaces. 2014; 6(23): 21730-21738.
[27] Ku SH, Park CB. Human endothelial cell growth on mussel-inspired nanofiber scaffold for vascular tissue engineering. Biomaterials. 2010; 31(36): 9431-9437.
[28] Pan F, Jia H, Qiao S, Jiang Z, Wang J, Wang B, et al. Bioinspired fabrication of high performance composite membranes with ultrathin defect-free skin layer. Journal of Membrane Science. 2009; 341(1): 279-285.
[29] Wei Q, Zhang F, Li J, Li B, Zhao C. Oxidant-induced dopamine polymerization for multifunctional coatings. Polymer Chemistry. 2010; 1(9): 1430-1433.

[30] Pan X-D, Qin Z, Yan Y-Y, Sadhukhan P. Elastomers with chain-end mussel-mimetic modification for nanocomposites: strong modifications to reinforcement and viscoelastic properties. Polymer. 2010; 51(15): 3453-3461.
[31] Hu M, Mi B. Enabling graphene oxide nanosheets as water separation membranes. Environmental Science & Technology. 2013; 47(8): 3715-3723.
[32] Gao H, Sun Y, Zhou J, Xu R, Duan H. Mussel-inspired synthesis of polydopamine-functionalized graphene hydrogel as reusable adsorbents for water purification. ACS Applied Materials & Interfaces. 2013; 5(2): 425-432.
[33] Sureshkumar M, Siswanto DY, Chen Y-C, Lee C-K, Wang M-J. Antibacterial and biocompatible surfaces based on dopamine autooxidized silver nanoparticles. Journal of Polymer Science Part B: Polymer Physics. 2013; 51(4): 303-310.
[34] Low WC, Rujitanaroj P-O, Lee D-K, Messersmith PB, Stanton LW, Goh E, et al. Nanofibrous scaffold-mediated REST knockdown to enhance neuronal differentiation of stem cells. Biomaterials. 2013; 34(14): 3581-3590.
[35] Kastner J, Pichler T, Kuzmany H, Curran S, Blau W, Weldon D, et al. Resonance Raman and infrared spectroscopy of carbon nanotubes. Chemical Physics Letters. 1994; 221(1): 53-58.
[36] Fei B, Qian B, Yang Z, Wang R, Liu WC, Mak CL, et al. Coating carbon nanotubes by spontaneous oxidative polymerization of dopamine. Carbon. 2008; 46(13): 1795-1797.
[37] Belin T, Epron F. Characterization methods of carbon nanotubes: a review. Materials Science and Engineering: B. 2005; 119(2): 105-118.
[38] Zhu J, Peng H, Rodriguez-Macias F, Margrave JL, Khabashesku VN, Imam AM, et al. Reinforcing epoxy polymer composites through covalent integration of functionalized nanotubes. Advanced Functional Materials. 2004; 14(7): 643-648.
[39] Liu W, Zhou R, Goh HL, Huang S, Lu X. From waste to functional additive: toughening epoxy resin with lignin. ACS Applied Materials & Interfaces. 2014; 6(8): 5810-5817.
[40] Yang S-Y, Ma C-CM, Teng C-C, Huang Y-W, Liao S-H, Huang Y-L, et al. Effect of functionalized carbon nanotubes on the thermal conductivity of epoxy composites. Carbon. 2010; 48(3): 592-603.

Scheme 1. The process of CNT functionalization and the formation of epoxy nanocomposites.

Fig. 1. TEM images of pristine CNTs (a), CNTs@PDA-25 (b), CNTs@PDA-10 (c), and CNTs@PDA-5 (d).

Fig. 2. FTIR spectra of DOPA, PDA, pristine CNTs, and CNTs@PDA.

Fig. 3. XRD profiles of pristine CNTs, CNTs@PDA-25, CNTs@PDA-10, and CNTs@PDA-5.

Fig. 4. TGA analysis of PDA, CNTs, CNTs@PDA-25, CNTs@PDA-10, and CNTs@PDA-5.

Fig. 5. Storage modulus versus temperature for the neat epoxy and PDA-coated CNT/epoxy nanocomposites.

Fig. 6. SEM images of neat epoxy (a,b), CNTs/EP (c,d), CNTs@PDA-25/EP (e,f), and CNTs@PDA-5/EP (g,h).

Fig. 7. TGA curves of neat epoxy, CNTs/EP, and composites with PDA-coated CNTs of varied PDA thickness.

Fig. 8. Thermal conductivity of CNTs/epoxy composites.

Fig.9. (a) SAXS and (b) WAXS measurements of composites containing CNTs of varying PDA layer thickness.

Scheme 1.

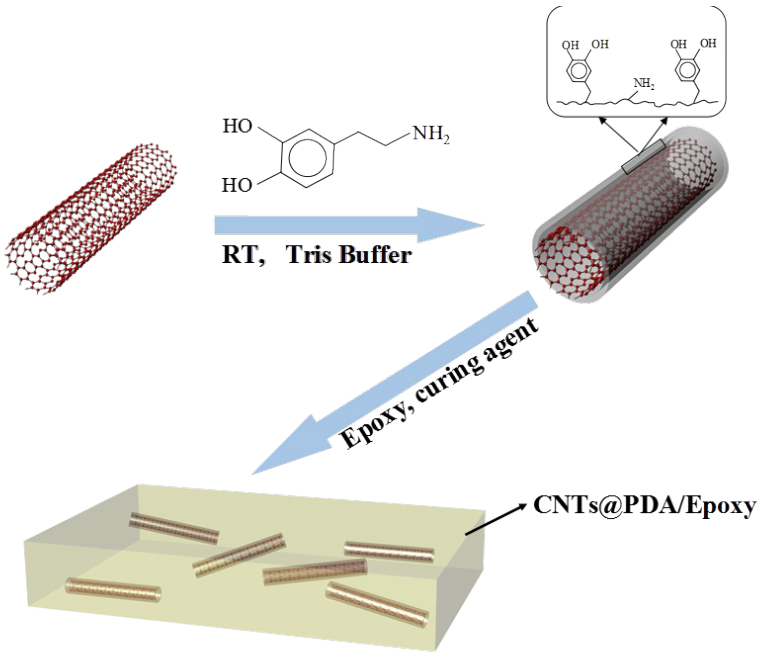

Fig.1.

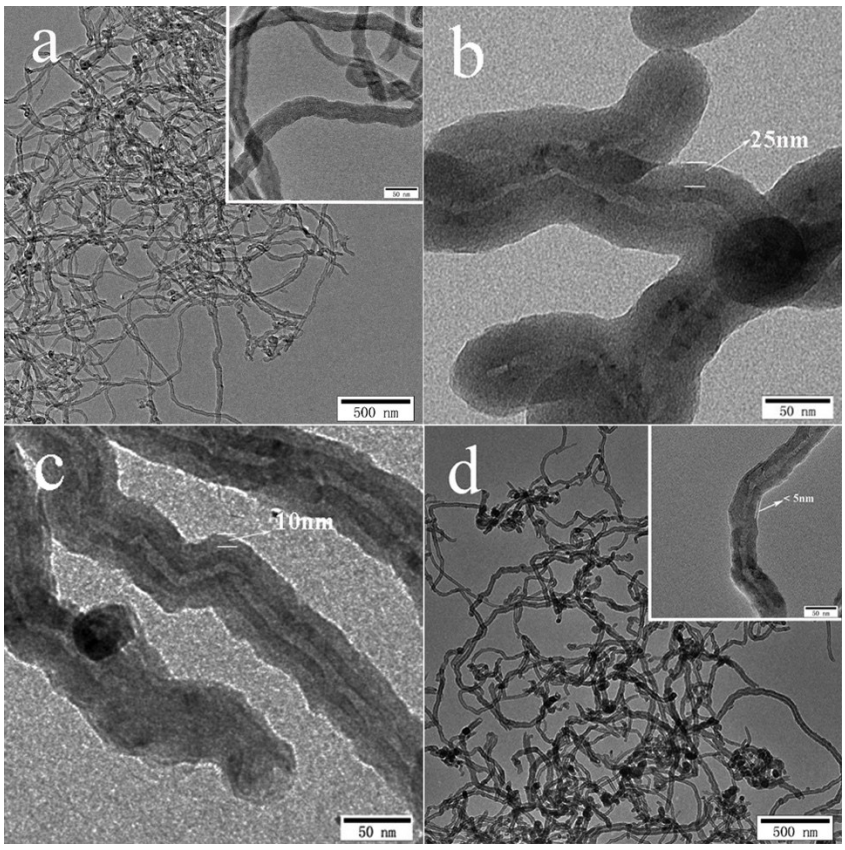
a
500 nm
b
25nm
50 nm
c
10nm
50 nm
d
< 5nm
500 nm

Fig.2.

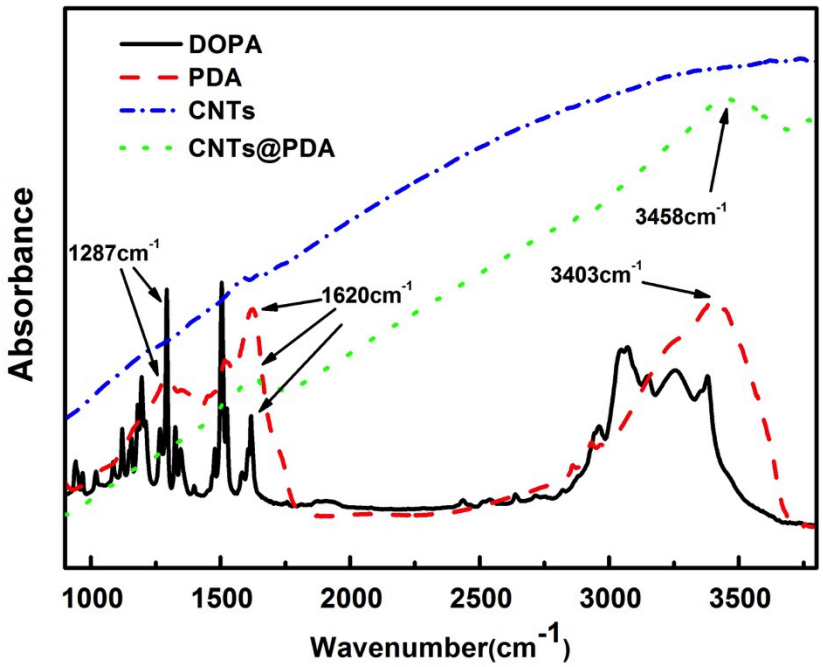
DOPA
PDA
CNTs
CNTs@PDA
Absorbance
1287cm-1
1620cm-1
3403cm-1
3458cm-1
1000
1500
2000
2500
3000
3500
Wavenumber(cm-1)

Fig.3.

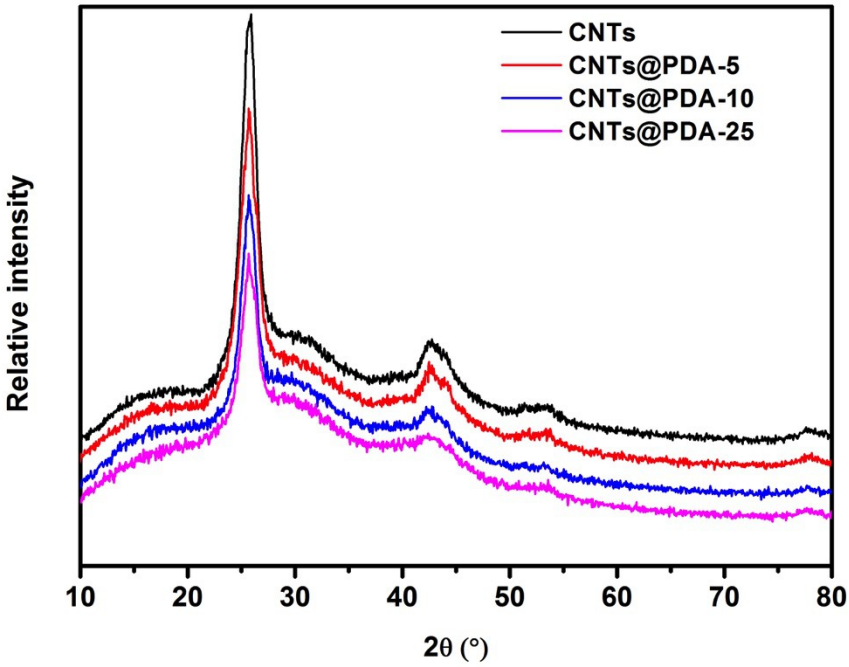
CNTs
CNTs@PDA-5
CNTs@PDA-10
CNTs@PDA-25
Relative intensity
10
20
30
40
50
60
70
80
2θ (°)

Fig.4.

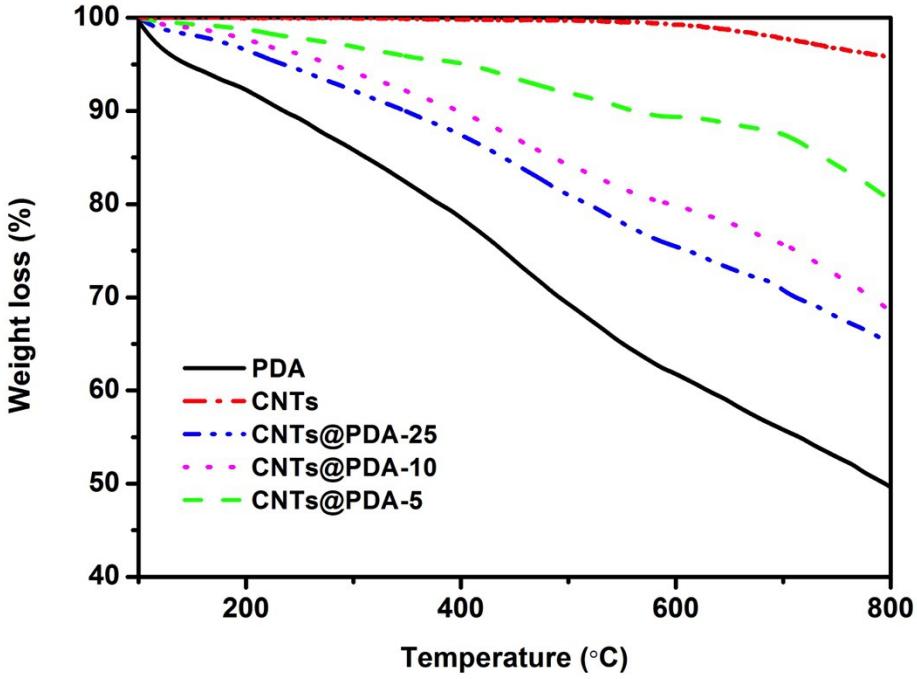
Weight loss (%)
Temperature (°C)
PDA
CNTs
CNTs@PDA-25
CNTs@PDA-10
CNTs@PDA-5

Fig.5.

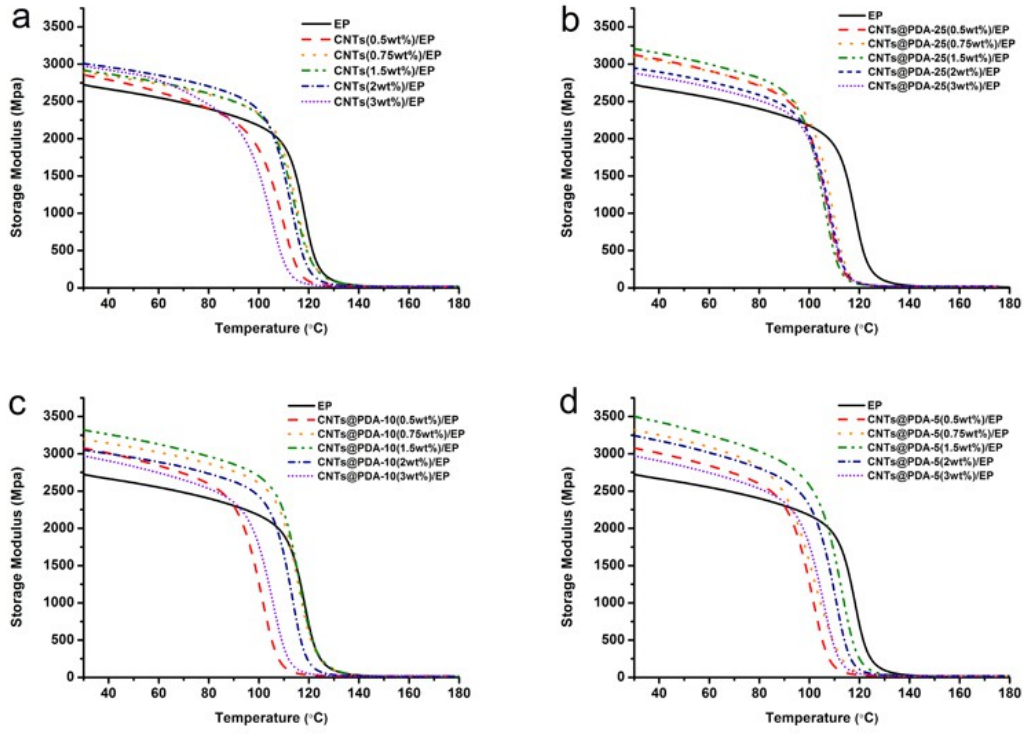
a
b
c
d
Storage Modulus (Mpa)
Temperature (°C)
EP
CNTs(0.5wt%)/EP
CNTs(0.75wt%)/EP
CNTs(1.5wt%)/EP
CNTs(2wt%)/EP
CNTs(3wt%)/EP
CNTs@PDA-25(0.5wt%)/EP
CNTs@PDA-25(0.75wt%)/EP
CNTs@PDA-25(1.5wt%)/EP
CNTs@PDA-25(2wt%)/EP
CNTs@PDA-25(3wt%)/EP
CNTs@PDA-10(0.5wt%)/EP
CNTs@PDA-10(0.75wt%)/EP
CNTs@PDA-10(1.5wt%)/EP
CNTs@PDA-10(2wt%)/EP
CNTs@PDA-10(3wt%)/EP
CNTs@PDA-5(0.5wt%)/EP
CNTs@PDA-5(0.75wt%)/EP
CNTs@PDA-5(1.5wt%)/EP
CNTs@PDA-5(2wt%)/EP
CNTs@PDA-5(3wt%)/EP

Fig.6.

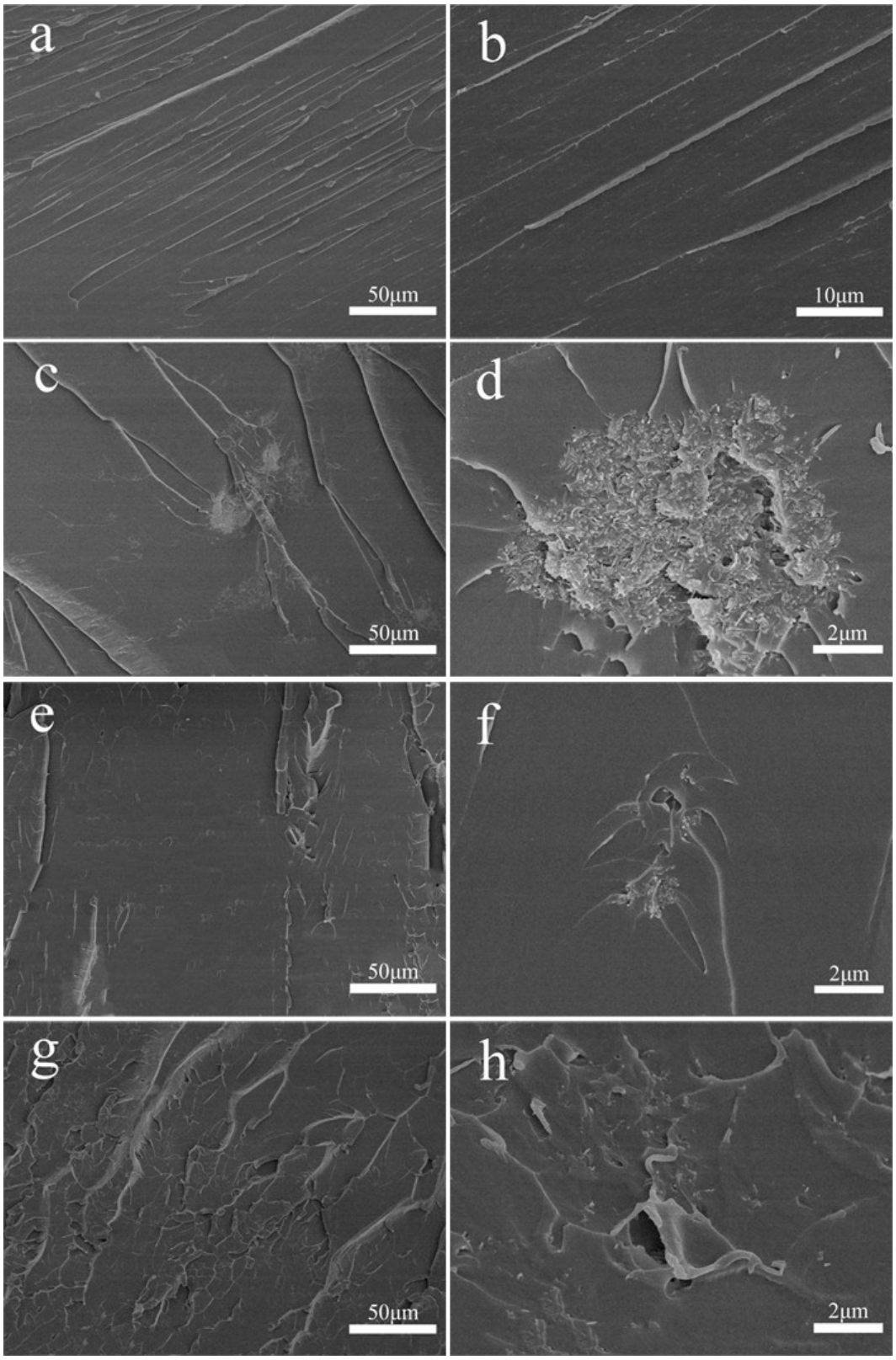

Fig.7.

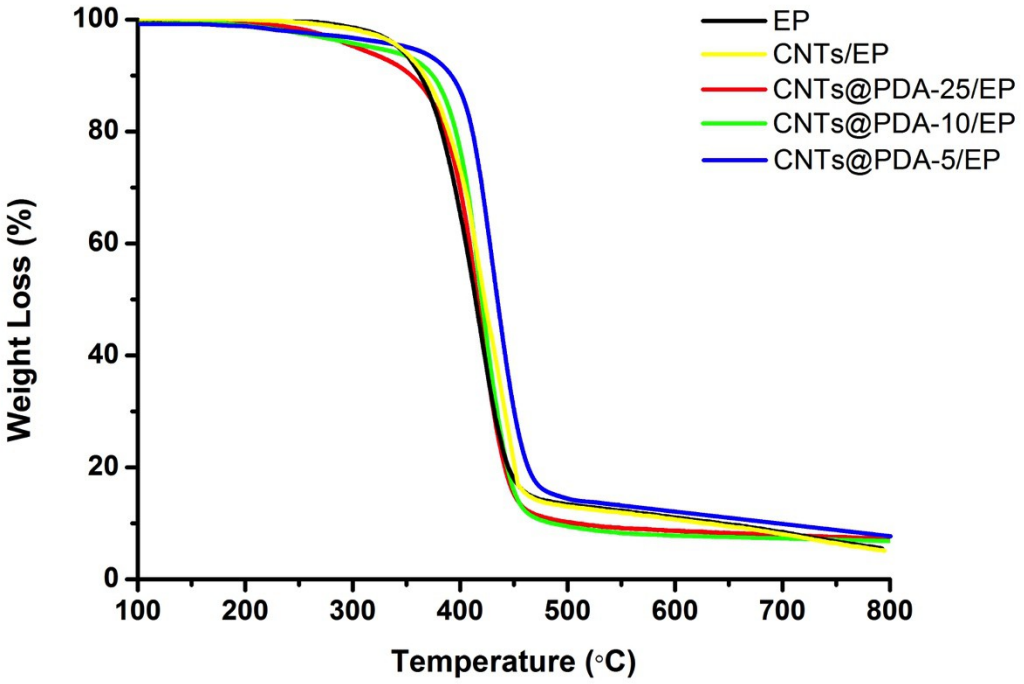
EP
CNTs/EP
CNTs@PDA-25/EP
CNTs@PDA-10/EP
CNTs@PDA-5/EP
Weight Loss (%)
Temperature (◦C)
100
80
60
40
20
0
100
200
300
400
500
600
700
800

Fig.8.

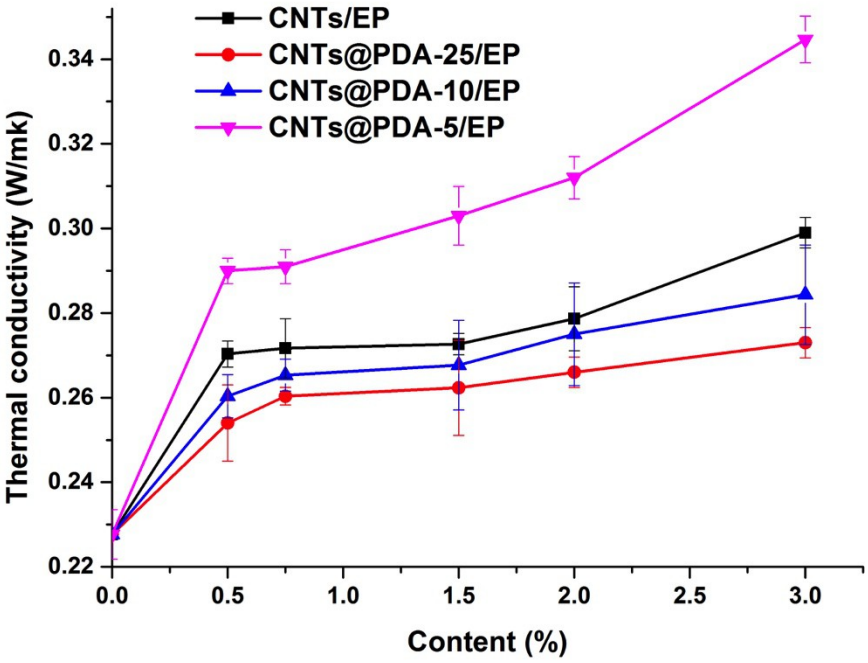

Fig. 9a and Fig. 9b

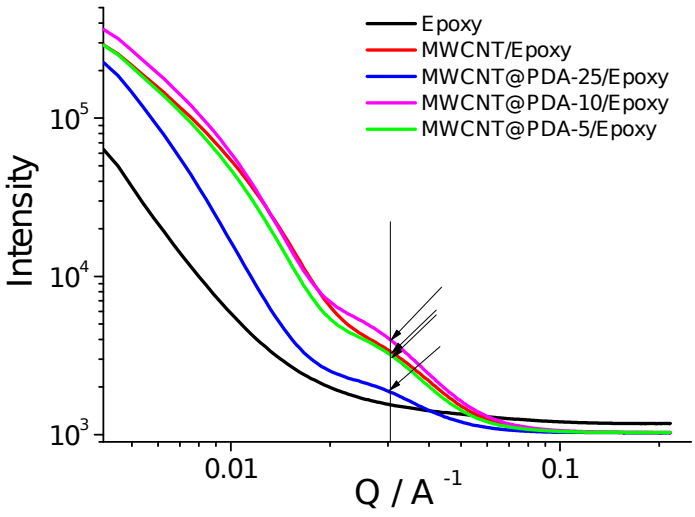

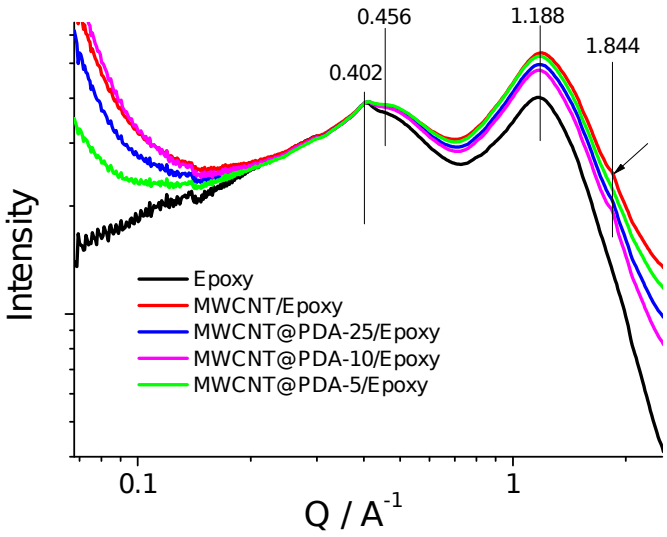

Table 1. Glass-transition temperature (T_g) of neat epoxy, CNTs/EP, CNTs@PDA-25/EP, CNTs@PDA-10/EP, and CNTs@PDA-5/EP.

Systems	0%	0.75%	1.5%	3%
CNTs/EP	125	123	124	115
CNTs@PDA-25/EP	125	118	118	118
CNTs@PDA-10/EP	125	124	125	114
CNTs@PDA-5/EP	125	118	123	114

Table 2. $T_{95wt\%}$ of epoxy composites containing CNTs of varying PDA coating thickness.

	EP	CNTs/EP	CNTs@PDA-25/EP	CNTs@PDA-10/EP	CNTs@PDA-5/EP
$T_{95wt\%}$(°C)	349	349	315	340	365